Aerothermodynamic Shape Optimization for Re-entry Capsule Using Genetic Algorithms

Ionut BUNESCU*,[1,2], Mihai-Victor PRICOP[1], Mihaita Gilbert STOICAN[1,2], Adrian Gheorghe DINA[2]

*Corresponding author
[1]INCAS – National Institute for Aerospace Research "Elie Carafoli",
B-dul Iuliu Maniu 220, 061126, Bucharest, Romania,
bunescu.ionut@incas.ro*, pricop.victor@incas.ro, stoican.gilbert@incas.ro
[2]"POLITEHNICA" University of Bucharest, Faculty of Aerospace Engineering,
Str. Gheorghe Polizu 1-7, 011061, Bucharest, Romania,
adii.george@yahoo.ro

DOI: 10.13111/2066-8201.2019.11.4.7

Received: 03 September 2019/ Accepted: 12 November 2019/ Published: December 2019

Abstract: *Space hasn't been for a long time now the final frontier, in the last years more and more spaceships have accessed outer space for different missions, some of them being required to return. The actual and main task of researchers is to find an optimal geometry for new generation of spacecraft which must be reusable and fit the imposed loads (heat flux, pressure, acceleration). The purpose of this paper is to optimize the design of a re-entry capsule configuration, in order to minimize the maximum heat flux on the thermal protection system and to obtain a wanted imposed drag coefficient. For the optimization process we use genetic algorithms and for the solving process, local inclination methods. Even if the latter are low-fidelity methods and do not offer satisfying results on all conditions, we consider them to be good enough for a preliminary study of an optimal design. Thus, this paper purpose is to describe the procedure to obtain an optimal configuration which can be better analyzed with high-fidelity methods.*

Key Words: *re-entry vehicles, local inclination methods, aerothermodynamic shape optimization*

1. INTRODUCTION

The recent space missions create the need to develop new re-entry capsules for different applications like space probes, space vehicles for transport, entry capsules for other planets or natural satellites. Each of these applications come with some requirements as stability, heat fluxes, deceleration factor, size, shape and others. In order to comply with all these requirements, the capsule configuration is needed to be optimized so that it achieves the required performance [1].

A modern tool for optimization problems is the genetic algorithm, although it has not been shown the convergence and the unicity of finding the global optimum, but for nonlinear optimization problems such as aerothermodynamic optimization it gave decent results at least for preliminary design. Optimization using genetic algorithm consists in evaluating several configurations for better results, of course, evaluating more configurations requires resources,

but using low-fidelity methods as local inclination methods, fast optimization can be achieved using decent resources [1, 9].

The local inclination methods are an important class of methods which can predict pressure coefficient distribution and heat flux distribution over a vehicle's surface based on vehicle's surface shape for hypersonic regimes. In principle, for estimation of heat flux or pressure coefficient over a surface we need two equations, first equation to predict the load in the stagnation point and the second one to predict the load over de surfaces based on the load in the stagnation point. In the present paper, the Modified Newton equation was used for pressure coefficient distribution and the Scott equation was used for heat flux distribution [3, 6]. In the following paragraphs these are shown:

$$C_{pS} = \frac{2}{\gamma M_\infty^2}\left[\left(\frac{(\gamma+1)^2 M_\infty^2}{4\gamma M_\infty^2 - 2(\gamma-1)}\right)^{\frac{\gamma}{\gamma-1}}\left(\frac{1-\gamma+2\gamma M_\infty^2}{\gamma+1}\right) - 1\right] \tag{1}$$

$$C_p = C_{pS}\sin^2\theta \tag{2}$$

The equations of estimation of pressure coefficient are given above; equation (1) represents the expression of pressure coefficient in the stagnation point and equation (2) represents the expression of pressure coefficient over the vehicle's surfaces, where θ represents the angle between the velocity vector and the reference plane of the local panel.

$$\dot{q}_S = 18{,}300\sqrt{\frac{\rho_\infty}{R_N}}\left(\frac{V_\infty}{10^4}\right)^{3.05} \tag{3}$$

$$\dot{q} = \dot{q}_S\cos\theta \tag{4}$$

The set of equations for estimation of heat flux distribution is represented above. Equation (3) represents the expression of heat flux in the stagnation point and equation (4) represents the expression of heat flux over the vehicle's surface [3, 4].

2. GEOMETRY PARAMETRIZATION

For the optimization process a parametrized geometry that can be easily updated in order to properly assist the localization of the optimum is required. In this case it's needed to find a way to create a geometry that depends of several parameters and that can be easily modified. The capsule geometry is an axis-symmetric surface, with an adequate generatrix, assembled by analytic curves as lines and circle arches. The front part of the capsule is made with circle arches and the back side of the capsule is made with straight lines, as in [1, 9]. The geometry parameterization which will be used in the optimization process is shown below:

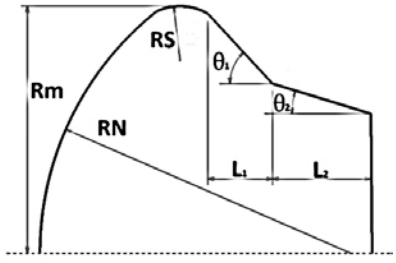

RN – nose radius
RS – side radius
θ_1 – First rear cone half angle
θ_2 – Second rear cone half angle
L_1 – First rear cone length
L_2 – Second rear cone length
Rm – Mid radius

Figure 1. Generatrix parametrization

The parameters from the figure above represent the values which can change the configuration of the vehicle. These parameters will be generated for each evaluation of the objective function along the optimization loop and the resulted geometry will be analyzed with local inclination methods [9].

3. CONSTRAINS AND PERFORMANCE CRITERIA

3.1 Constrains

The geometry presented above depends on some parameters, but without limits lower and upper bounds for the parameters, the capsule can have some unnatural shapes. Thus, in order to eliminate these cases, a certain constraint on the parameters and performances must be imposed. To constraint the parameters, a range of values where they can vary according to regular re-entry capsules for each of them are set:

Table 1. - Values range for geometry parameters

Parameter	Minimum Value	Maximum Value
RN	4000 mm	6000 mm
RS	200 mm	500 mm
θ_1	-45°	45°
θ_2	-45°	45°
L_1	750 mm	1200 mm
L_2	750 mm	1200 mm
Rm	1500 mm	2500 mm

Besides of geometry parameters, a nonlinear constraint over the capsule's performances like the load factor and the volumetric efficiency as in Table 2 must be imposed.

Table 2. Performances constraints

Volumetric efficiency:	$\eta_V = 6\sqrt{\pi}\frac{V}{S^{3/2}}$	$\eta_V \in [1.65, 2.3]$
Load factor:	$n = \frac{\frac{1}{2}\rho v^2 S\sqrt{C_L^2 + C_D^2}}{mg}$	$n \in [0, 8]$

These constraints guarantee that the geometry configuration search space will only sweep through feasible geometries that satisfy the imposed limits [1, 2].

3.2 Performance Criteria

Because any optimization problem needs an objective function, some performance criteria must be established to optimize the process. Many performance criteria are chosen to see how the optimal geometry configuration depends on them [1, 2].

Most of the time in a re-entry mission, the very important aerothermodynamic performance criteria are the drag coefficient, the heat flux and the stability, therefore some optimizations with these criteria combined in an objective function will be performed [1, 2].

In this paper four optimization problems are solved which are presented below:

Minimizing the heat flux $$f_q = Q_{max} \quad (5)$$

Increasing the stability $$f_x = 1/x_{cp} \quad (6)$$

Maximizing drag coefficient $f_D = 1/C_D$ (7)

Increasing aerothermodynamic performances $f_{mixt} = \frac{1}{\left(\frac{C_D}{C_{Dref}} + \frac{x_{cp}}{x_{cpref}} + \frac{q_{maxref}}{q_{max}}\right)}$ (8)

References values from equation (8) are obtained for the case of sphere, in the following table:

$C_{Dref} = 0.98$	$x_{cpref} = 0.3027$	$q_{maxref} = 925.45\ W/cm^2$

First case (5), minimization of heat flux must find the optimal geometry configuration for the minimum heat flux in the stagnation point for a thin and light thermal protection system. Second case (6), increasing the stability must offer optimal geometry configuration for the maximum stability, where the distance between the capsule's nose and the center of pressure is maximum.

The third case (7), maximization of drag coefficient must offer the optimal geometry configuration for the maximum drag coefficient but not exceeding load factor constraints, this performance criterion is important for aerodynamic deceleration. The fourth case (8) incorporates a linear combination between the above-mentioned performance criteria for a global optimum configuration.

4. AEROTHERMODYNAMIC OPTIMIZATION

After establishing the geometry parameterization, variables lower and upper bounds, nonlinear constraints, aerodynamic model and optimization model, we can perform the optimization cases for each performance criteria can be performed. In the following section each case, their optimization process and results will be presented [2].

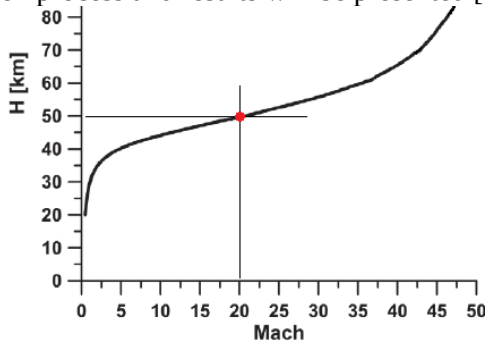

H = 50 km
M = 20
$\alpha \in [0°, 10°]$

Figure 2. Flight condition

A specific case of re-entry capsules will be considered, meeting the following requirements: no radiative heat flux, predominantly laminar flow and continuum regime, these requirements being specific for 50 km altitude and 20 Mach number. Figure 2 presents an ordinary dependency Mach number - altitude for re-entry capsules, where the red point represents the case which we will perform [6, 7].

4.1 Minimizing the heat flux

The main advantage of minimal heat flux on the vehicle surface is a thin and light thermal protection system which means that launcher performances increase, while the payload mass decreases, the required amount of fuel decreases and the TPS volume decreases as well, so that resources can be saved for the same requirements.

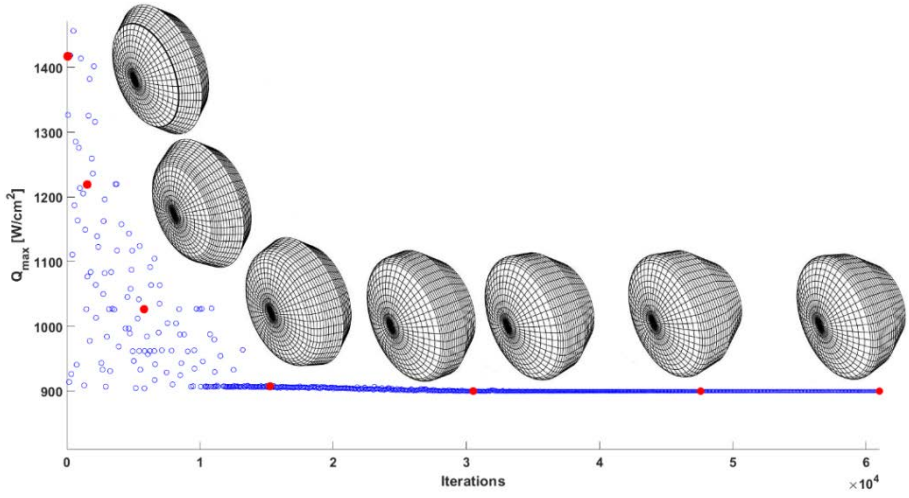

Figure 3. Optimization evolution for minimal heat flux case

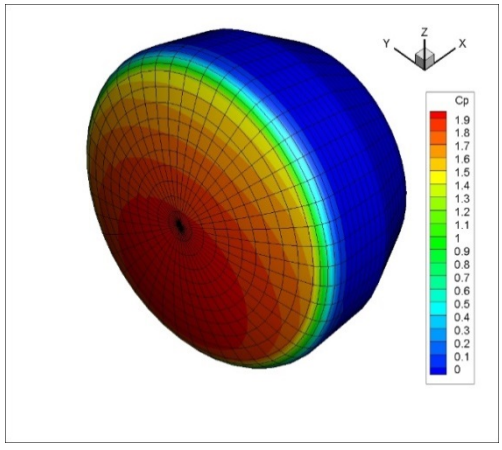

Figure 4. Pressure coefficient distribution for minimal heat flux case

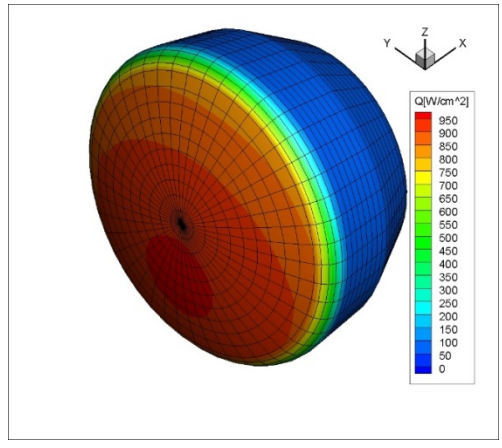

Figure 5. Heat flux distribution for minimal heat flux case

For this case a population of individuals equal to 200 was chosen and the stall limit was reached at the 315th generation. So, in this case, 63000 function evaluations (FEs) were performed as it can be seen in Figure 3 which presents the evolution of the capsule geometry during the optimization process. After the optimization process, the optimization variables vector from Figure 1 has been obtained:

P = [5999.98; 388.2; 8.4; 37.2; 2488.2; 990.8; 959.1]

The geometry of optimized capsule for minimum heat flux can be seen in Figure 4 and Figure 5 where the pressure coefficient distribution and the heat flux distribution over the capsule surface are presented. It can be observed that the heat flux in the stagnation point is around to 950 W/cm^2. This geometry configuration is very similar to Soyuz and Dragon re-entry capsules [5].

4.2 Maximizing the stability

A good stability for the re-entry capsules is required to avoid tumble and implicit capsules destruction. Small motion disturbances affect the capsule trajectory and therefore it is very

important to have a margin of stability. A good stability for the re-entry capsules is given by the distance between the stagnation point and the center of pressure.

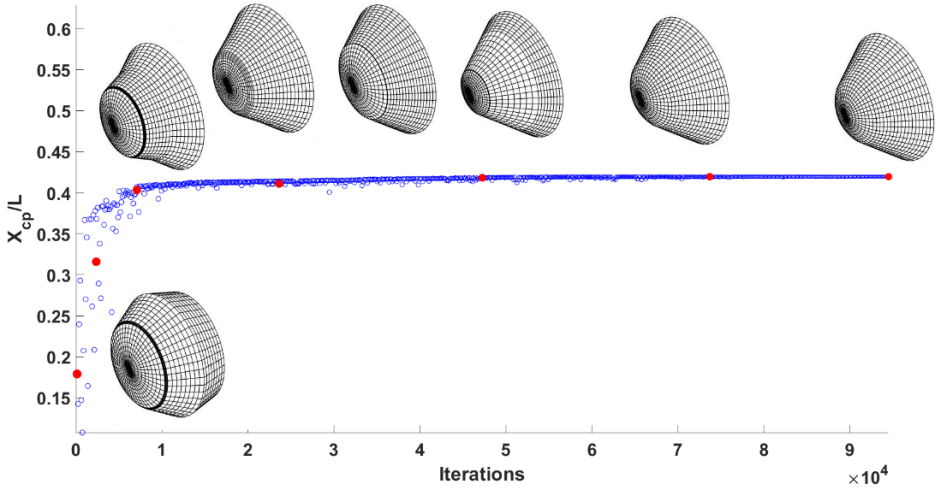

Figure 6. Optimization evolution for maximal stability case

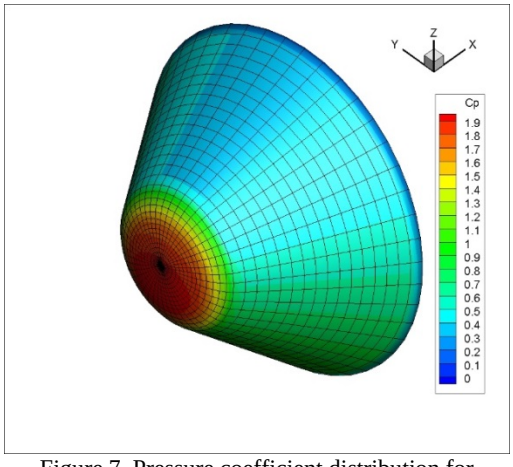

Figure 7. Pressure coefficient distribution for maximal stability case

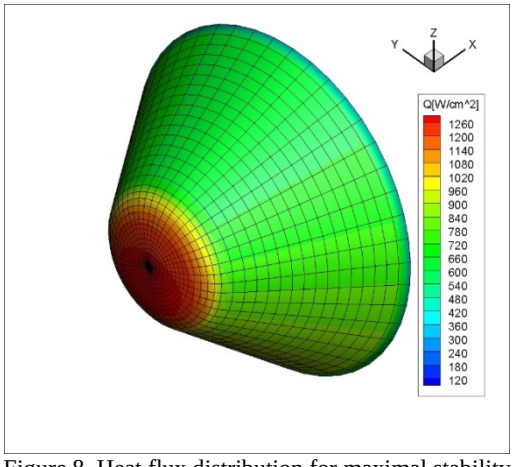

Figure 8. Heat flux distribution for maximal stability case

In this case of optimization, a population of 200 individuals was chosen and the stall limit was reached at the 468th generation such that in this case 93600 FEs were performed as it can be seen in Figure 6, where the evolution of the capsule geometry during the optimization process is presented. The optimization variables vector resulted from this optimization process is given below:

P = [4012.2; 201.5; -44.9; -45; 1501.2; 1156.1; 1198.1]

The geometry of optimized capsule for maximum stability can be observed in Figure 7 and Figure 8 where the pressure coefficient distribution and heat flux distribution on the capsule surface are presented. A highlighted result is the heat flux in the stagnation point which is around 1260 W/cm^2. This geometry configuration is very similar to Huygens probe and Orex demonstrator [5].

4.3 Maximizing drag coefficient

For many re-entry capsules or probes which are not equipped with special air deceleration system it is very important to have a high drag coefficient, but for manned capsules it is very important not to exceed a limit load factor for crew's safety.

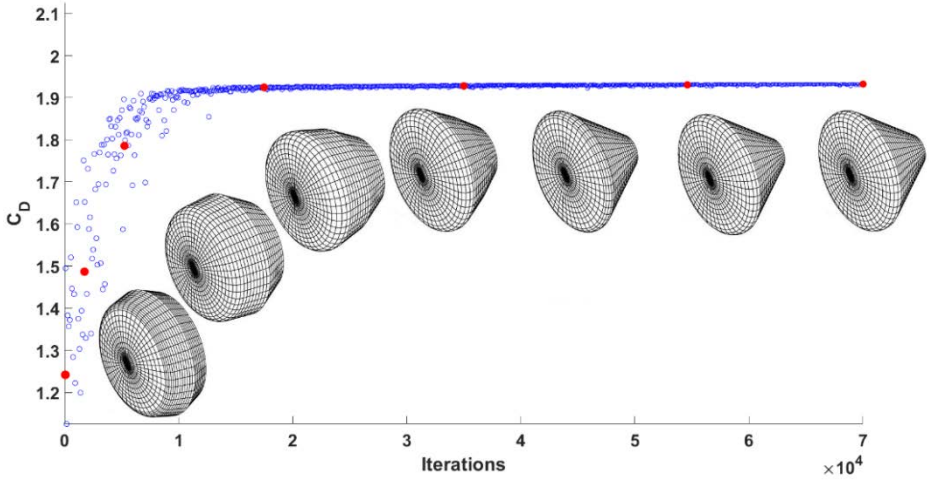

Figure 9. Optimization evolution for maximum drag coefficient case

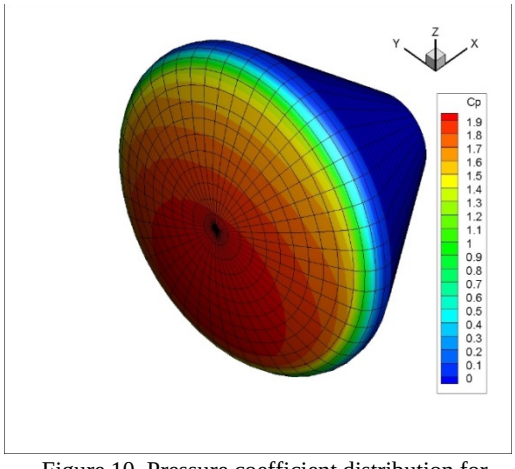

Figure 10. Pressure coefficient distribution for maximal drag coefficient case

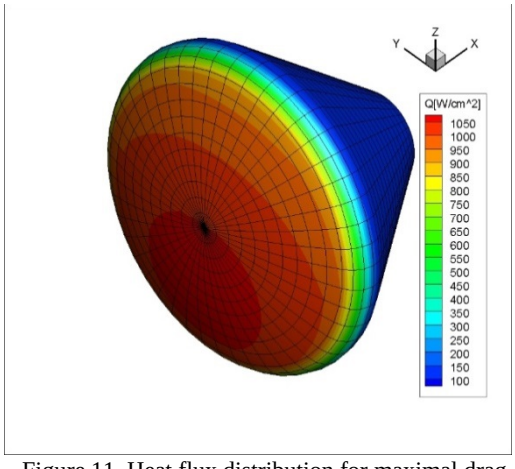

Figure 11. Heat flux distribution for maximal drag coefficient case

For this case a population of individuals equal to 200 was chosen and the stall limit was reached at the 348th generation so in this case 69600 FEs were performed as we can see in Figure 9, where the evolution of the capsule geometry during the optimization process is presented. After the optimization process, the following solution vector has been obtained:

P = [5998.8; 389.5; 44.1; 43.2; 2489.6; 1186.5; 1178.3]

The geometry of the optimized capsule for maximum drag coefficient can be seen in Figure 10 and Figure 11, where the pressure coefficient distribution and heat flux distribution on the capsule surface are presented. It can be observed that the pressure coefficient is predominantly high in the front and the heat flux in the stagnation point is around 1050W/cm^2. This geometry configuration is very similar to that of Apollo and ARD capsule [5].

4.4 Minimizing linear combination

The actual need is to design a capsule geometry that meets several requirements such as high drag coefficient, high stability and low heat flux.

Two types of multi-disciplinary optimization can be performed: a combined objective function and a multi-objective function.

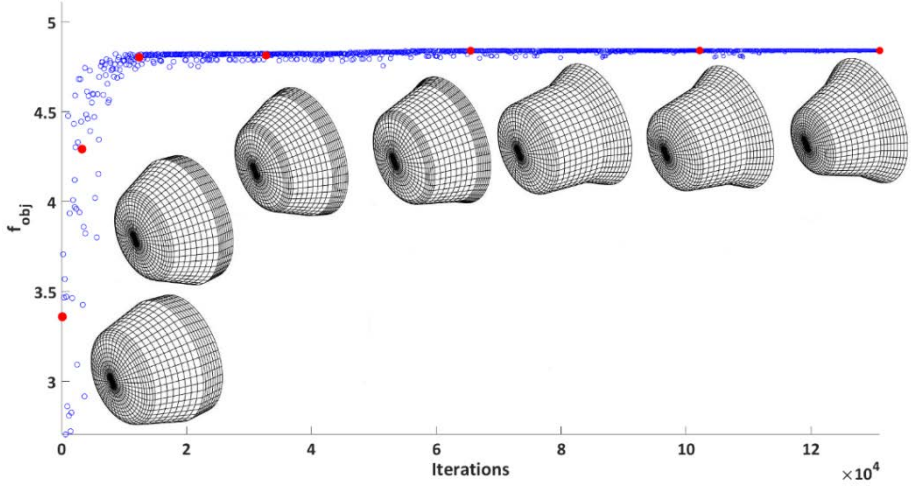

Figure 12. Optimization evolution for combined case

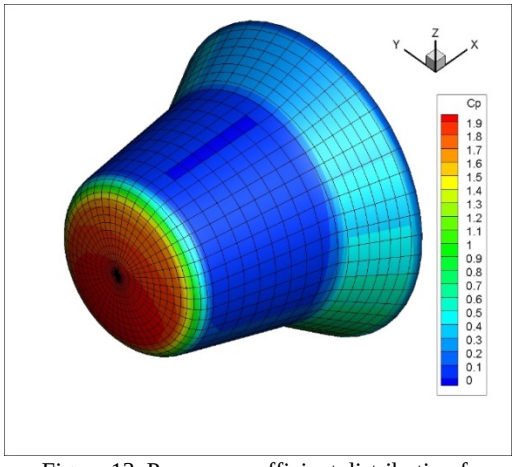

Figure 13. Pressure coefficient distribution for combined case

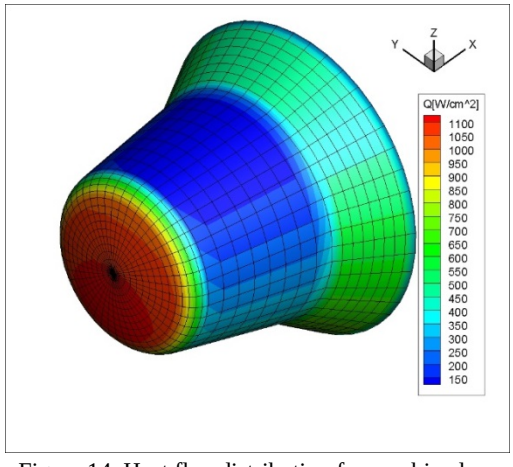

Figure 14. Heat flux distribution for combined case

For this final case a population of individuals equal to 1000 was chosen for a good searching; the stall limit was reached at 132th generation, so in this case 132000 FEs were performed as it can be seen in Figure 12 which presents the evolution of the capsule geometry during the optimization process.

After the optimization process, the solution vector has been obtained and it is shown below:

P = [4002.3; 209.1; -9.1; -44.8; 1649.6; 1186.5; 778.3]

The geometry of the optimized capsule for the combined case can be seen in Figure 13 and Figure 14 presenting the pressure coefficient distribution and heat flux distribution over the capsule surface.

5. CONCLUSIONS

We can conclude that local inclination methods represent a good tool in aerothermodynamic optimization because it provides decent results very fast and the usage of genetic algorithm in aerothermodynamic optimization can provide a good localization of at the global minimum.

This work encourages us to develop optimization tools for more complex re-entry vehicles as lifting bodies or winged bodies. An important improvement which can be performed for the optimization problems with multi-objective functions is to use pareto front.

REFERENCES

[1] D. Dirkx, E. Mooij, *Conceptual shape optimization of entry vehicles*, Springer, 2017.
[2] A. Viviani, G., Pezzella, *Aerodynamic and Aerothermodynamic Analysis of Space Mission Vehicles*, Springer, 2015.
[3] M. V. Pricop, I. C. Andrei, M. Boscoianu, Application of Modified Newton Flow Model to Reentry Capsules, *INCAS BULLETIN*, Vol. **6**, Special issue 1, (online) ISSN 2247–4528, (print) ISSN 2066–8201, ISSN–L 2066–8201, DOI: 10.13111/2066-8201.2014.6.S1.14, pp. 129-134, 2014.
[4] M. C. Fadgyas, M. V. Pricop, M. L. Niculescu, M. G. Cojocaru, A. Dumitrache, Semi-empirical relations for pressure distributions in hypersonic regime, *AIP Conference Proceedings*, Vol. **1978**, Issue 1, 2018.
[5] C. Weiland, *Aerodynamic Data of Space Vehicles*, Springer, 2014.
[6] J. D. Anderson, *Hypersonic and High Temperature Gas Dynamics*, Second Edition, AIAA Education, 2006.
[7] W. D. Hayes, R. F. Probstein, *Hypersonic Flow Theory I: Inviscid Flows*, Second Edition, Academic Press, New York, 1966.
[8] D. Dirkx, E. Mooij, Continuous aerodynamic modelling of entry shapes, *AIAA Journal*, AIAA-2011-6575, 2011.
[9] D. Dirkx, E. Mooij, Optimization of entry-vehicle shapes during conceptual design, *Acta Astronautica*, 2014.
[10] J. Fuller, R. Tolson, Improved methods for estimation of spacecraft free-molecular aerodynamic properties, *Journal of Spacecraft and Rockets*, **46**(5), 2009.